The Cryosphere, 11, 1733–1743, 2017
https://doi.org/10.5194/tc-11-1733-2017

The Cryosphere Open Access EGU

Experimental observation of transient $\delta^{18}O$ interaction between snow and advective airflow under various temperature gradient conditions

Pirmin Philipp Ebner[1], **Hans Christian Steen-Larsen**[2,3], **Barbara Stenni**[4], **Martin Schneebeli**[1], **and Aldo Steinfeld**[5]

[1]WSL Institute for Snow and Avalanche Research SLF, 7260 Davos Dorf, Switzerland
[2]LSCE Laboratoire des Sciences du Climat et de l'Environnement, Gif-Sur-Yvette CEDEX, France
[3]Center for Ice and Climate, Niels Bohr Institute, University of Copenhagen, Copenhagen, Denmark
[4]Department of Environmental Sciences, Informatics and Statistics, University Ca' Foscari of Venice, Venice, Italy
[5]Department of Mechanical and Process Engineering, ETH Zurich, 8092 Zurich, Switzerland

Correspondence to: Martin Schneebeli (schneebeli@slf.ch)

Received: 9 February 2017 – Discussion started: 20 February 2017
Revised: 31 May 2017 – Accepted: 9 June 2017 – Published: 25 July 2017

Abstract. Stable water isotopes ($\delta^{18}O$) obtained from snow and ice samples of polar regions are used to reconstruct past climate variability, but heat and mass transport processes can affect the isotopic composition. Here we present an experimental study on the effect of airflow on the snow isotopic composition through a snow pack in controlled laboratory conditions. The influence of isothermal and controlled temperature gradient conditions on the $\delta^{18}O$ content in the snow and interstitial water vapour is elucidated. The observed disequilibrium between snow and vapour isotopes led to the exchange of isotopes between snow and vapour under non-equilibrium processes, significantly changing the $\delta^{18}O$ content of the snow. The type of metamorphism of the snow had a significant influence on this process. These findings are pertinent to the interpretation of the records of stable isotopes of water from ice cores. These laboratory measurements suggest that a highly resolved climate history is relevant for the interpretation of the snow isotopic composition in the field.

1 Introduction

Water stable isotopes in polar snow and ice have been used for several decades as proxies for global and local temperatures (e.g. Dansgaard, 1964; Lorius et al., 1979; Grootes et al., 1994; Petit et al., 1999; Johnsen et al., 2001; EPICA Members, 2004). However, the processes that influence the isotopic composition of precipitation at high latitudes are complex, making direct inference of palaeotemperatures from the isotopic record difficult (Cuffey et al., 1994; Jouzel et al., 1997, 2003; Hendricks et al., 2000). Several factors affect the vapour and snow isotopic composition, which give rise to ice-core isotopic composition, starting from the process of evaporation in the source region, transportation of the air mass to the top of the ice sheet and post-depositional processes (Craig and Gordon, 1964; Merlivat and Jouzel, 1979; Johnsen et al., 2001; Ciais and Jouzel, 1994; Jouzel and Merlivat, 1984; Jouzel et al., 2003; Helsen et al., 2005, 2006, 2007; Cuffey and Steig, 1998; Krinner and Werner, 2003). Mechanical processes such as mixing, seasonal scouring or spatial redistribution of snow can alter seasonal and annual records (Fisher et al., 1983; Hoshina et al., 2014). Post-depositional processes associated with wind scouring and snow redistribution are known to introduce a "post-depositional noise" in the surface snow. Comparisons of isotopic records obtained from closely located shallow ice cores have allowed for estimations of a signal-to-noise ratio and a common climate signal (Fisher and Koerner, 1988, 1994; White et al., 1997; Steen-Larsen et al., 2011; Sjolte et al., 2011; Masson-Delmotte et al., 2015). After deposition, interstitial diffusion in the firn and ice affects the water-isotopic signal but back-diffusion or deconvolution techniques have been used to establish the original isotope signal (Johnsen, 1977; Johnsen et al., 2000).

Snow is a bicontinuous material consisting of fully connected ice crystals and pore space (air) (Löwe et al., 2011). Because of the proximity to the melting point, the high vapour pressure causes a continuous recrystallization of the snow microstructure known as snow metamorphism, even under moderate temperature gradients (Pinzer et al., 2012). The whole ice matrix is continuously recrystallizing by sublimation and deposition, with vapour diffusion as the dominant transport process. Pinzer et al. (2012) showed that a typical half-life of the ice matrix is a few days. The intensity of the recrystallization is dictated by the temperature gradient and this can occur under midlatitude or polar conditions. Temperature and geometrical factors (porosity and specific surface area) also play a significant role (Pinzer and Schneebeli, 2009; Pinzer et al., 2012).

The interpretation of ice-core data and the comparison with atmospheric model results implicitly rely on the assumption that the snowfall precipitation signal is preserved in the snow–ice matrix (Werner et al., 2011). Classically, ice-core stable-isotope records are interpreted as reflecting precipitation-weighted signals and compared to observations and atmospheric model results for precipitation, ignoring exchanges between surface snow and atmospheric water vapour (e.g. Persson et al., 2011). However, recent studies carried out on top of the Greenland and Antarctic ice sheets combining continuous atmospheric water-vapour-isotope observations with daily snow surface sampling document a clear day-to-day variation of isotopic composition of surface snow between precipitation events as well as diurnal change in the snow isotopes (Steen-Larsen et al., 2014a; Ritter et al., 2016; Casado et al., 2016). This effect was interpreted as being caused by the uptake of the synoptic-driven atmospheric water-vapour-isotope signal by individual snow crystals undergoing snow metamorphism (Steen-Larsen et al., 2014a) and the diurnal variation in moisture flux (Ritter et al., 2016). However, the impact of this process on the isotope-temperature reconstruction is not yet sufficiently understood, but crucial to constrain. This process, compared to interstitial diffusion (Johnsen, 1977; Johnsen et al., 2000), will alter the isotope mean value. The field observations challenge the previous assumption that sublimation occurred layer-by-layer with no resulting isotopic fractionation (Dansgaard, 1964; Friedman et al., 1991; Town et al., 2008; Neumann and Waddington, 2004). It is assumed that the solid undergoing sublimation would not be unduly enriched in the heavier isotope species due to the preferential loss of lighter isotopic species to the vapour (Dansgaard, 1964; Friedman et al., 1991). Because self-diffusion in the ice is about 3 orders of magnitude slower than molecular diffusion in the vapour, the amount of isotopic separation in snow is assumed to be negligible.

Snow has a high permeability (Calonne et al., 2012; Zermatten et al., 2014), which facilitates diffusion of gases and, under appropriate conditions, airflow (Gjessing, 1977; Colbeck, 1989; Sturm and Johnson, 1991; Waddington et al., 1996). In a typical Antarctic and Greenland snow profile, strong interactions between the atmosphere and snow occur, especially in the first 2 m (Neumann and Waddington, 2004; Town et al., 2008), called the convective zone. In the convective zone, air can move relatively freely and therefore exchange occurs between snow and the atmospheric air. Air flowing into the snow reaches saturation vapour pressure nearly instantly through sublimation (Neumann et al., 2008; Ebner et al., 2015a). Models of the influence of the so-called "wind pumping" effect (Fisher et al., 1983; Neumann and Waddington, 2004), in which the interstitial water vapour is replaced by atmospheric air pushed through the upper metres of the snow pack by small-scale high and low pressure areas caused by irregular grooves or ridges formed on the snow surface (dunes and sastrugi), have assumed that the snow grains would equilibrate with the interstitial water vapour on timescales governed by ice self-diffusion. However, no experimental data are available to support this assumption. With this in mind the experimental study presented here is specifically developed to investigate the effect of ventilation inside the snow pack on the isotopic composition. Only conditions deeper than 1 cm inside a snowpack are considered. Previous work showed that (1) under isothermal conditions, the Kelvin effect leads to a saturation of the pore space in the snow but does not affect the structural change (Ebner et al., 2015a), (2) applying a negative temperature gradient along the flow direction leads to a change in the microstructure due to deposition of water molecules on the ice matrix (Ebner et al., 2015b), and (3) a positive temperature gradient along the flow had a negligible total mass change of the ice but a strong reposition effect of water molecules on the ice grains (Ebner et al., 2016). Here, we continuously measured the isotopic composition of an airflow containing water vapour through a snow sample under both isothermal and temperature gradient conditions. Microcomputed-tomography (μCT) was applied to obtain the 3-D microstructure and morphological properties of snow.

2 Experimental set-up

Isothermal and temperature gradient experiments with fully saturated airflow and defined isotopic composition were performed in a cold laboratory at around $T_{\mathrm{lab}} \approx -15\,^{\circ}\mathrm{C}$ with small fluctuations of $\pm 0.8\,^{\circ}\mathrm{C}$ (Ebner et al., 2014). Snow produced from de-ionized tap water in a cold laboratory (water temperature: $30\,^{\circ}\mathrm{C}$; air temperature: $-20\,^{\circ}\mathrm{C}$) was used for the snow sample preparation (Schleef et al., 2014). The snow was sieved with a mesh size of 1.4 mm into a box and isothermally sintered for 27 days at $-5\,^{\circ}\mathrm{C}$ to increase the strength in order to prevent destruction of the snow sample due to the airflow and to evaluate the effect of metamorphism of snow. The morphological properties of the snow are listed in Table 1. The sample holder (diameter 53 mm, height 30 mm, 0.066 L) was filled by a cylinder cut out from the sintered

Table 1. Morphological properties and flow characteristics of the experimental runs: µCT measured snow density (ρ), porosity (ε), specific surface area per unit mass (SSA), mean pore space diameter (d_{mean}), superficial velocity in snow (u_D), corresponding Reynolds number ($Re = d_{\text{mean}} \cdot u_D/\nu_{\text{air}}$), average inlet temperature of the humidifier and at the inlet ($T_{\text{in, mean}}$), average outlet temperature at the outlet ($T_{\text{out, mean}}$) and average temperature gradient (∇T_{ave}). Experiment (1) corresponds to the isothermal conditions, experiment (2) to air warming and experiment (3) to air cooling in the snow sample.

	ρ kg m^{-3}	ε –	SSA m^2 kg^{-1}	d_{mean} mm	u_D m s^{-1}	Re –	$T_{\text{in, mean}}$ °C	$T_{\text{out, mean}}$ °C	∇T_{ave} K m^{-1}
Experiment (1)	202	0.78	28	0.39	0.03	0.76	−15.5	−15.5	–
Experiment (2)	202	0.78	30	0.36	0.03	0.70	−15.4	−14.0	+47
Experiment (3)	220	0.76	27	0.37	0.031	0.74	−12.3	−14.1	−60

snow. To prevent airflow between the snow sample and the sample holder walls, the undisturbed snow disk was filled in at a higher temperature (about −5 °C) and sintering was allowed for about 1 h before cooling down at the start of the experiment. The set-up of Ebner et al. (2014) was modified by additionally inserting a water-vapour-isotope analyser (model: L1102-I Picarro, Inc., Santa Clara, CA, USA) to measure the isotopic ratio δ^{18}O of the water vapour contained in the airflow at the inlet and outlet of the sample holder. The experimental set-up consisted of three main components (humidifier, sample holder and the Picarro analyser) connected with insulated copper tubing and Swagelok fitting (Fig. 1). The tubes to the Picarro analyser were heated to prevent deposition of water vapour and thereby fractionation. The temperature was monitored with thermistors inside the humidifier and at the inlet and outlet of the snow sample. A dry air pressure tank controlled by a mass flow controller (EL-Flow, Bronkhorst) generated the airflow. A humidifier, consisting of a tube (diameter 60 mm, height 150 mm, 0.424 L volume) filled with crushed ice particles (snow from Antarctica with low δ^{18}O composition), was used to saturate the dry air entering the humidifier with water vapour at an almost constant isotopic composition. The air temperature in the humidifier and at the inlet of the snow sample was maintained at the same value (accuracy ±0.2 K) to limit the influence of variability in absolute vapour pressure and isotopic composition. We measured the δ^{18}O of the water vapour produced by the humidifier before and after each experimental run ($\delta^{18}O_{\text{hum}}$). The outlet flow ($\delta^{18}O_a$) of the sample holder was continuously measured during the experiment to analyse the temporal evolution of the isotopic signal. All data from the Picarro analyser were corrected to the humidity reference level using the established instrument humidity-isotope response (Steen-Larsen et al., 2013, 2014b). In addition, VSMOW-SLAP correction and drift correction were performed. We followed the calibration protocol and used the calibration system described in detail by Steen-Larsen et al. (2013, 2014b).

The sample holder described by Ebner et al. (2014) was used to analyse the snow by µCT. Tomography measurements were performed with a modified µ-CT80 (Scanco Medical). The equipment incorporated a microfocus X-ray

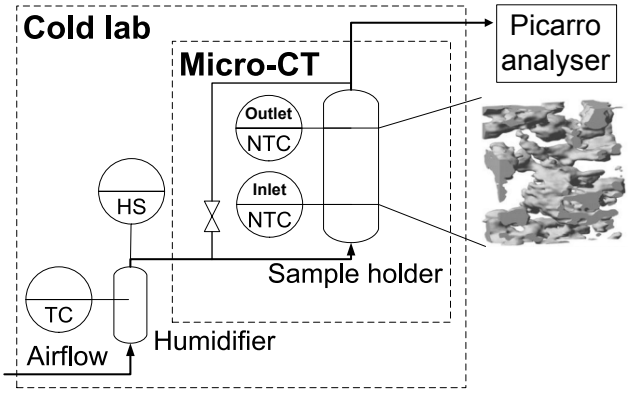

Figure 1. Schematic of the experimental set-up. A thermocouple (TC) and a humidity sensor (HS) inside the humidifier measured the mean temperature and humidity of the airflow. Two thermistors (NTC) close to the snow surface measured the inlet and outlet temperature of the airflow (Ebner et al., 2014). The Picarro analyser measured the isotopic composition δ^{18}O of the outlet flow. Inset: 3-D structure of $110 \times 42 \times 110$ voxels ($2 \times 0.75 \times 2\,\text{mm}^3$) obtained by the µCT.

source, operated at 70 kV acceleration voltage with a nominal resolution of 18 µm. The samples were scanned with 1000 projections per 180° in high-resolution setting, with typical adjustable integration time of 200 ms per projection. The field of view of the scan area was 36.9 mm of the total 53 mm diameter and subsamples with a dimension of $7.2 \times 7.2 \times 7.2\,\text{mm}^3$ were extracted for further processing. The reconstructed µCT images were filtered using a $3 \times 3 \times 3$ median filter followed by a Gaussian filter ($\sigma = 1.4$, support = 3). The Otsu method (Otsu, 1979) was used to automatically perform clustering-based image thresholding to segment the grey-level images into ice and void phase. Morphological properties in the two-phase system were determined based on the exact geometry obtained by the µCT. Tetrahedrons corresponding to the enclosed volume of the triangulated ice matrix surface were applied to the segmented data to determine porosity (ε) and specific surface area (SSA). The mean pore size distribution was estimated using the opening-size-distribution operation. This operation can be imagined as

Table 2. δ^{18}O is the vapour in the humidifier ($\delta^{18}O_{hum}$) and of the snow in the sample holder ($\delta^{18}O_s$) at the beginning ($t = 0$) and end ($t =$ end) of each experiment and the final δ^{18}O content of the snow in the sample holder at the inlet ($z = 0$ mm) and outlet ($z = 30$ mm). Experiment (1) corresponds to the isothermal conditions, experiment (2) to air warming and experiment (3) to air cooling in the snow sample.

	$\delta^{18}O_{hum}$ ‰		$\delta^{18}O_s$, $t = 0$ ‰	$\delta^{18}O_{s,t=end}$ ‰	
	$t = 0$	$t =$ end		$z = 0$ mm	$z = 30$ mm
Experiment (1)	−68.2	−67.5	−10.97	−17.75	−15.72
Experiment (2)	−66.3	−66.1	−11.94	−19.60	−16.60
Experiment (3)	−62.8	−62.2	−10.44	−25.53	−15.00

virtual sieving with different mesh sizes (Haussener et al., 2012).

Three experiments with saturated advective airflow through the snow sample were performed to record the following parameters and analyse their effects: (1) isothermal conditions to analyse the influence of curvature effects (Kaempfer al et., 2007), (2) positive temperature gradient applied to the snow sample where cold air entering the sample is heated while flowing through the sample in order to analyse the influence of sublimation, and (3) negative temperature gradient applied to the snow sample where warm air entering the sample is cooled while flowing across the sample to analyse the influence of net deposition. During the temperature gradient experiments, temperature differences of 1.4 and 1.8 °C were imposed, resulting in gradients of +47 and $-60\,\mathrm{K\,m^{-1}}$, respectively. The runs were performed at atmospheric pressure and with a volume flow rate of $3.0\,\mathrm{L\,min^{-1}}$ corresponding to an average flow speed in the pores of $u_D \approx 30\,\mathrm{mm\,s^{-1}}$. We performed the experiments with airflow velocities in the snow sample at $u_D \approx 30\,\mathrm{mm\,s^{-1}}$, which is a factor of 3 higher than calculated by Neumann (2003) for a natural snow pack. However, when looking at the Reynolds number and describing the flow regime inside the pores, our experiments ($Re \approx 0.7$) were in the feasible flow regime (laminar flow) of a natural snow pack ($Re \approx 0.65$). The outlet temperature in experiment (2) and the inlet and the humidifier temperature in experiment (3) were actively controlled using thermo-electric elements. Variations in temperature of up to ±0.8 °C were due to temperature fluctuations inside the cold laboratory, leading to slightly variable temperature gradients and mean temperature in experiment (2) and (3). Table 1 presents a summary of the experimental conditions and the morphological properties of the snow samples. All snow samples were taken from the same snow block with an average density of $\approx 210\,\mathrm{kg\,m^{-3}}$. The density given in Table 1 was the density of the snow sample in each experiment measured by µCT. At the end of each experiment, the snow sample was cut into five layers of 6 mm height and the isotopic composition of each layer was analysed to examine the spatial δ^{18}O gradient in the isotopic composition of the snow sample.

A slight increase with a maximum of 0.7 ‰ of δ^{18}O in the water vapour produced by the humidifier was observed in experiment (1), with lower increases during experiments (2) and (3) (Table 2). This change of ~ 0.7 ‰ is not significant compared to the difference between the isotopic composition of the water vapour and the snow sample in the sample holder of ~ 53 ‰ and the temporal change of the water-vapour isotopes on the back side of the snow sample.

In approximately the first 30 min, the isotopic composition of the measured outflow air $\delta^{18}O_a$ increased from a low δ^{18}O to a starting value of around −29 ‰ in each experiment. This was due to a memory effect and another possible effect might be condensed water left in the tubes from a prior experiment which had no further impact on the experiments (Penna et al., 2012).

3 Results

3.1 Isothermal condition

Experiment (1) was performed for 24 h at a mean temperature of $T_{mean} = -15.5$ °C. $\delta^{18}O_a$ decreased exponentially in the outlet flow observed throughout the experimental run as shown in Fig. 2. Initially, the $\delta^{18}O_a$ content in the flow was −27.7 ‰ and exponentially decreased to −47.6 ‰ after 24 h. The small fluctuations in the $\delta^{18}O_a$ signal at $t \approx 7$, 17 and 23 h were due to small temperature changes in the cold laboratory.

We observed a strong interaction between the airflow and the snow as manifest by the isotopic composition of the snow. The $\delta^{18}O_s$ signal in the snow decreased by 4.75–7.78 ‰ and an isotopic gradient in the snow was observed after the experimental run, shown in Fig. 3. Initially, the snow had a homogeneous isotopic composition of $\delta^{18}O_s = -10.97$ ‰ but post-experiment sampling showed a decrease in the snow δ^{18}O at the inlet side to −17.75 ‰ and at the outlet side to −15.72 ‰. The spatial $\delta^{18}O_s$ gradient of the snow had an approximate slope of $0.68\,\text{‰}\,\mathrm{mm^{-1}}$ at the end of the experimental run. Table 2 shows the δ^{18}O value in snow at the beginning ($t = 0$) and end ($t = 24$ h) of the experiment.

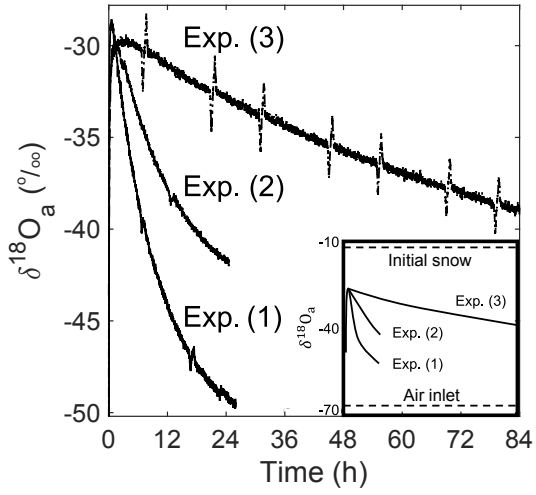

Figure 2. Temporal isotopic composition of δ^{18}O of the outflow for each of the experimental runs. The spikes in the δ^{18}O were due to small temperature changes in the cold laboratory (Ebner et al., 2014). Exp. (1) corresponds to the isothermal conditions, Exp. (2) to air warming and Exp. (3) to air cooling in the snow sample. The higher the recrystallization rate of the snow the slower the adaption of δ^{18}O of the outlet air to the inlet air. The illustration in the lower right corner shows the relation between δ^{18}O of the initial snow, inlet and outlet of the air.

3.2 Air warming by a positive temperature gradient along the airflow

Experiment (2) was performed over a period of 24 h with an average temperature gradient of approximatively $+47\,\mathrm{K\,m^{-1}}$ (warmer temperatures at the outlet of the snow) and an average mean temperature of $-14.7\,^{\circ}\mathrm{C}$. As in the isothermal experiment (1), we observed a relaxing exponential decrease of $\delta^{18}O_a$ in the outlet flow throughout the measurement period as shown in Fig. 2, but the decrease was slower compared to the isothermal run. Initially, the $\delta^{18}O_a$ content in the flow coming through the snow disk was $-29.8\,‰$ and exponentially decreased to $-41.9\,‰$ after 24 h. The small fluctuations in the $\delta^{18}O_a$ signal at $t \approx 2.7$ and 12.7 h were due to small temperature changes in the cold laboratory.

The $\delta^{18}O_s$ signal in the snow decreased by 4.66–7.66 ‰ and a gradient in the isotopic composition of the snow was observed after the experimental run, shown in Fig. 3. Initially, the snow had a homogeneous isotopic composition of $\delta^{18}O_s = -11.94\,‰$, but post-experiment sampling showed a decrease at the inlet side to $-19.6\,‰$ and at the outlet side to $-16.6\,‰$. The spatial $\delta^{18}O_s$ gradient of the snow had an approximate slope of $1.0\,‰\,\mathrm{mm^{-1}}$ at the end of the experimental run. Table 2 shows the $\delta^{18}O_s$ values in snow at the beginning ($t = 0$) and end ($t = 24$ h) of the experiment.

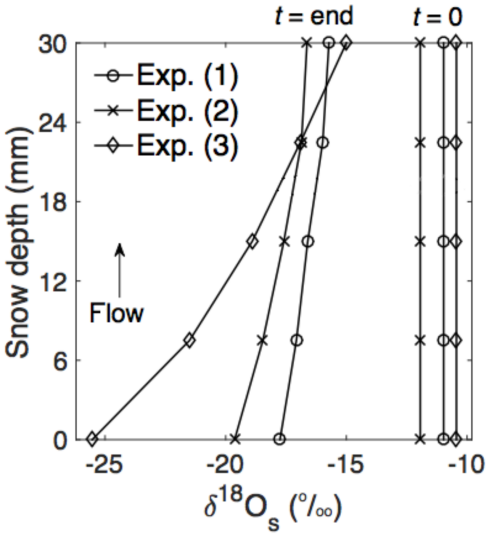

Figure 3. Spatial isotopic composition of δ^{18}O of the snow sample at the beginning ($t = 0$) and at the end ($t =$ end) for each experiment. The air entered at $z = 0$ mm and exited at $z = 30$ mm. Exp. (1) corresponds to the isothermal conditions Exp. (2) to air warming and Exp. (3) to air cooling in the snow sample.

3.3 Air cooling by a negative temperature gradient along the airflow

Experiment (3) was performed for 84 h instead of 24 h to better estimate the trend in $\delta^{18}O_a$ in the outlet flow. An average temperature gradient of approximately $-60\,\mathrm{K\,m^{-1}}$ (colder temperatures at the outlet of the snow) and an average mean temperature of $-13.2\,^{\circ}\mathrm{C}$ were observed during the experiment. As in the previous experiments, a relaxing exponential decrease of $\delta^{18}O_a$ in the outlet flow was observed throughout the experimental run as shown in Fig. 2. The decrease was slower compared to experiments (1) and (2). Initially, the $\delta^{18}O_a$ content in the flow was $-29.8\,‰$ and exponentially decreased to $-37.7\,‰$ after 84 h. The small fluctuations in the $\delta^{18}O_a$ signal at $t \approx 7.3$, 21.3, 31.3, 45.3, 55.3, 69.3 and 79.3 h were due to small temperature changes in the cold laboratory.

The $\delta^{18}O_s$ signal in the snow decreased by 4.46–15.09 ‰ and a gradient in the isotopic composition of the snow was observed after the experimental run, shown in Fig. 3. Initially, the snow had an isotopic composition of $\delta^{18}O_s = -10.44\,‰$ but post-experiment sampling showed a decrease at the inlet side to $-25.53\,‰$ and at the outlet side to $-15.00\,‰$. The spatial $\delta^{18}O_s$ gradient of the snow had an approximate slope of $3.5\,‰\,\mathrm{mm^{-1}}$ at the end of the experimental run. Table 2 shows the $\delta^{18}O_s$ value in snow at the beginning ($t = 0$) and end ($t = 84$ h) of the experiment.

4 Discussion

All experiments showed a strong exchange in δ^{18}O between the snow and water-vapour-saturated air, resulting in a significant change in the values of the stable isotopes in the snow. The advective conditions in the experiments were comparable with surface snow layers in Antarctica and Greenland, but at higher temperatures, especially compared to the interior of Antarctica.

The results also showed strong interactions in δ^{18}O between snow and air depending on the different temperature gradient conditions. The experiments indicate that temperature variation and airflow above and through the snow structures (Sturm and Johnson, 1991; Colbeck, 1989; Albert and Hardy, 1995) seem to be dominant processes affecting water stable isotopes of surface snow. The results also support the statement that an interplay occurs between theoretically expected layer-by-layer sublimation and deposition at the ice-matrix surface and the isotopic content evolution of snow cover due to mass exchange between the snow cover and the atmosphere (Sokratov and Golubev, 2009). The specific surface area of snow exposed to mass exchange (Horita et al., 2008) and by the depth of the snow layer exposed to the mass exchange with the atmosphere (He and Smith, 1999) plays an important role. Our results support the interpretation that changes in surface snow isotopic composition are expected to be significant if large day-to-day surface changes in water vapour occur in between precipitation events, wind pumping is efficient and snow metamorphism is enhanced by temperature gradients in the upper first centimetres of the snow (Steen-Larsen et al., 2014a).

We expect that our findings will lead to an improvement of the interpretation of the water stable-isotope records from ice cores. Classically, ice-core stable-isotope records are interpreted as palaeotemperature, reflecting precipitation-weighted signals. When comparing observations and atmospheric model results for precipitation with ice-core records, such snow–vapour exchanges are normally ignored (e.g. Persson et al., 2011; Fujita and Abe, 2006). However, snow–vapour exchange enhanced by recrystallization rate seems to be an important factor for the high variation in the snow surface δ^{18}O signal as supported by our experiments. It was hypothesized that the changes in the snow-surface δ^{18}O reported by Steen-Larsen et al. (2014a) are caused by changes in large-scale wind and moisture advection of the atmospheric water-vapour signal and snow metamorphism. The strong interaction between atmosphere and near-surface snow can modify the ice-core water stable-isotope records.

The rate-limiting step for isotopic exchange in the snow is isotopic equilibration between the pore-space vapour and surrounding ice grains. The relaxing exponential decrease of δ^{18}O in the outflow of our experiments predicted that full isotopic equilibrium between snow and atmospheric vapour will not be reached at any depth (Waddington et al., 2002; Neumann and Waddington, 2004) but changes move towards equilibrium with the atmospheric state (Steen-Larsen et al., 2013, 2014a).

As snow accumulates, the upper 2 m are advected through the ventilated zone (Neumann and Waddington, 2004; Town et al., 2008). In areas with high accumulation rate (e.g. South Greenland), snow is advected for a short time through the ventilated zone. The snow exposed for a relatively short time to vapour snow exchange would result in higher spatial variability compared to longer exposure. However, the effects of snow ventilation on isotopic composition may become more important as the accumulation rate of the snow decreases ($< 50\,\mathrm{mm\,a^{-1}}$), such that snow remains in the near-surface ventilated zone for many years (Waddington et al., 2002; Hoshina et al., 2014, 2016). As the snow remains for a longer time in the near-surface ventilated zone, a larger δ^{18}O exchange will occur between snow and atmospheric vapour. Consequently, the isotopic content of layers at sites with high and low accumulation rates can evolve differently, even if the initial snow composition had been equal, and the sites had been subjected to the same histories of air-mass vapour.

Despite a relatively small change in the difference between the isotopic composition of the incoming vapour and the snow, large differences in the isotopic composition of the water vapour at the outlet flow exist for the three different experimental set-ups. Based on the difference in the outlet water-vapour isotopic composition, we hypothesized that different processes are at play for the different experiments. It is obvious that there is a fast isotopic exchange with the surface of the ice crystals and a much slower timescale on which the interior of the ice crystals is altered. Due to the low diffusivity of $H_2{}^{16}O$ and $H_2{}^{18}O$ in ice ($D_{H_2{}^{18}O} \approx D_{H_2{}^{16}O} = \sim 10^{-15}\,\mathrm{m^2\,s^{-1}}$ (Ramseier, 1967; Johnsen et al., 2000), we assumed that the interior of the ice crystals is not altered on the timescale of the experiment. This explained why the net isotopic change of the bulk sample is relatively small compared to the changes in the outlet water-vapour isotopes. The effective "ice-diffusion depth" of the isotopic exchange during the experiments is given as $L_D = \sqrt{D \cdot t}$, where D is the diffusion coefficient of $H_2{}^{16}O$ and $H_2{}^{18}O$ in ice and t is the experimental time. The calculated ice-diffusion depth L_D, is $\sim 9.3\,\mu\mathrm{m}$ for experiments (1) and (2), and $\sim 17.4\,\mu\mathrm{m}$ for experiment (3), respectively, indicating an expected a minimal change of the interior of the ice crystal. However, snow has a large specific surface area and therefore a high exchange area. This has an effect on the δ^{18}O snow concentration. The fraction of the total volume V_{tot} of ice that is close enough to the ice surface to be affected by diffusion in time t is then $\rho_{\mathrm{ice}} \cdot \mathrm{SSA} \cdot L_D$, where SSA is the specific surface area (area per unit mass), and L_D is the diffusion depth, defined above, for time t. For $t \approx 24\,\mathrm{h}$, a large fraction (24 to 43 %) of the total volume V_{tot} of the ice matrix can be accessed through diffusion. It is quite hard to see the total δ^{18}O snow difference between experiments (1) and (2) after the experiment compared to the δ^{18}O of the vapour in the air at the outlet.

There is a small but notable difference in the total δ^{18}O of the snow between experiments (1) and (2). Due to the higher recrystallization rate of experiment (2) the spatial $\delta^{18}O_s$ gradient of the snow ($1.0\,‰\,mm^{-1}$) is higher than for experiment (1) ($0.68\,‰\,mm^{-1}$). Increasing the experimental time, the δ^{18}O change in the snow increases (experiment 3). In general, the calculated ice-diffusion depth is realistic under isothermal conditions where diffusion processes are the main factors (Kaempfer and Schneebeli, 2007; Ebner et al., 2015). By applying a temperature gradient, the impact of diffusion is suppressed due to the high recrystallization rate by sublimation and deposition. Due to the low half-life of a few days of the ice matrix, the growth rates are typically of the order of $100\,\mu m\,day^{-1}$ (Pinzer et al., 2012). Therefore, this redistribution of ice caused by temperature gradient counteracts the diffusion into the solid ice.

By comparing similarities and differences between the outcomes of the three experimental set-ups we will now discuss the physical processes influencing the interaction and exchange processes within the snowpack between the snow and the advected vapour. We first notice that the final snow isotopic profiles of experiments (1) (isothermal) and (2) (positive temperature gradient along the direction of the flow) are comparable to each other. Despite this similarity, the evolution in the outlet water vapour of experiment (1) showed a significantly stronger depletion compared to experiment (2). For experiment (3) (negative temperature gradient along the direction of the flow) we observed the smallest change in outlet water-vapour isotopes but the largest snowpack isotope gradient after the experiment. However, this change was caused by 84 h flow instead of 24 h.

Curvature effects, temperature gradients and therefore the recrystallization rate influence the mass transfer of $H_2{}^{16}O/H_2{}^{18}O$ molecules. The higher the recrystallization rate of the snow the slower the adaption of the outlet air concentration to the inlet air concentration (see in experiments 2 and 3). Under isothermal conditions (experiment 1) the only effect influencing the recrystallization rate is the curvature effect (Kaempfer and Schneebeli, 2007). However, based on the experimental observations (Kaempfer and Schneebeli, 2007) this effect decreases with decreasing temperature and increasing experimental time. Applying an additional temperature gradient to a snow sample causes complex interplays between local sublimation and deposition on surfaces and the interaction of water molecules in the air with the ice matrix due to changing saturation conditions of the airflow. Therefore, the recrystallization rate increases and causes the change in the δ^{18}O of the air. For experiment (2) there is a complex interplay between sublimation and deposition of water molecules into the interstitial flow (Ebner et al., 2015c), while for experiment (3) there is deposition of molecules carried by the interstitial flow onto the snow crystals (Ebner et al., 2015b). Furthermore, in the beginning of each experiment there is a tendency to sublimate from edges of the individual snow crystals due to the higher curvature. As the edges were sublimated and deposition occurred in the concavities, the individual snow crystals became more rounded, slowing down the transfer of water molecules into the interstitial airflow. We noticed, for all three experiments, that within the uncertainty of the isotopic composition of the snow, the initial isotopic composition of the vapour was the same and in isotopic equilibrium with the snow. The difference between experiments (1) and (2) lies in the fact that due to the temperature gradient in experiment (2) there is an increased transfer of water vapour with the isotopic composition of the snow into the airflow. Hence the depleted air from the humidifier advected through the snow disk is mixed with a relatively larger vapour flux from the snow crystals. Additionally, we also expected less deposition into the concavities in experiment (2) compared to experiment (1). However, it is interesting to note that the final isotopic profile of the snow disk is similar in experiment (1) and experiment (2). We interpreted this as being a result of two processes acting in opposite directions: although relatively isotope-depleted vapour from the humidifier was deposited onto the ice matrix there was also a higher amount of sublimation of relatively isotope-enriched vapour from the snow disk in experiment (2). Experiment (3) separates itself from the other two experiments in that as the water vapour from the humidifier is advected through the snow disk there is a continuous deposition of very depleted air due to the negative temperature gradient. As for experiments (1) and (2) there was also a constant sublimation of the convexities into the vapour stream in experiment (3). We notice that, despite the fact that experiment (3) ran for 84 h, the snow at the outlet side of the snow disk did not become more isotopically depleted compared to experiments (1) and (2). However, the snow on the inlet side became significantly more isotopically depleted. This observation, together with the fact that the vapour of the outlet of the snow disk is less depleted compared to experiments (1) and (2), leads us to hypothesize that there is a relatively larger deposition of isotopically depleted vapour from the humidifier as the vapour is advected through the snow disk. This means that a relatively larger component of the isotopic composition of the vapour is originating by sublimation from the convexities of the snow disk and a smaller one from the isotopically depleted vapour from the humidifier.

Our results and conclusions indicate that there is a need for additional validation. Specifically, it would be crucial to know the mass balance of the snow disk more precisely, which could be done by reconstructing the entire snow disk following the change in density and morphological properties over the entire height. Ideally, the entire sample would be tomographically measured with a resolution of $4\times4\times4\,mm^3$, each cube corresponding to the representative volume. Insights would also be achieved with experiments using snow of the same isotopic composition, but different SSA, as a more precise calculation of the different observed exchange rates would be allowed. Additionally, different and colder background temperatures should be tested to better under-

stand the inland Antarctic environment and the effect of the quasi-liquid layer, which is necessary for the development of a numerical model. Isotopically different combinations of vapour and snow should be performed. In the present paper, vapour with low δ^{18}O isotopic composition was transported through snow with relative high δ^{18}O isotopic composition. It would be interesting to reverse the combination and perform experiments with different combinations to provide more insights on mass and isotope exchanges between vapour and snow. Experiments with longer running time help to understand the change in the ice matrix better under low accumulation conditions.

5 Summary and conclusion

Laboratory experimental runs were performed where a transient δ^{18}O interaction between snow and air was observed. The airflow altered the isotopic composition of the snowpack and supports an improved climatic interpretation of ice core stable water-isotope records. The water-vapour-saturated airflow with an isotopic difference of up to 55 ‰ changed the original δ^{18}O isotope signal in the snow by up to 7.64 and 15.06 ‰ within 24 and 84 h. The disequilibrium between snow and air isotopes led to the observed exchange of isotopes, the rate depending on the temperature gradient conditions. To conclude, increasing the recrystallization rate in the ice matrix causes the temporal change of the δ^{18}O concentration at the outflow to decrease (experiment 2 and 3). Decreasing the recrystallization rate causes the temporal curve of the outlet concentration to become steeper, reaching the δ^{18}O inlet concentration of the air faster (experiment 1).

Additionally, the complex interplay of simultaneous diffusion, sublimation and deposition due to the geometrical complexity of snow has a strong effect on the δ^{18}O signal in the snow and cannot be neglected. A temporal signal can be superimposed on the precipitation signal, (a) if the snow remains near the surface for a long time, i.e. in a low-accumulation area, and (b) if it is exposed to a history of air masses carrying vapour with a significantly different isotopic signature than the precipitated snow.

These are novel measurements and will therefore be important as the basis for further research and experiments. Our results represent direct experimental observations of the interaction between the water isotopic composition of the snow, the water vapour in the air and recrystallization due to temperature gradients. Our results demonstrate that recrystallization and bulk mass exchange must be incorporated into future models of snow and firn evolution. Further studies are required on the influence of temperature and airflow as well as on snow microstructure on the mass transfer phenomena for validating the implementation of stable water isotopes in snow models.

Data availability. All data are available at https://doi.org/10.16904/20 (EnviDat.ch data portal).

Competing interests. The authors declare that they have no conflict of interest.

Acknowledgements. The Swiss National Science Foundation granted financial support under project Nr. 200020-146540. Hans Christian Steen-Larsen was supported by the AXA Research Fund. The authors thank Koji Fujita, Edwin Waddington and an anonymous reviewer for the suggestions and critical review. Matthias Jaggi, Sascha Grimm, Alessandro Schlumpf and Sarah Berben gave technical support. The data for this paper are available by contacting the corresponding author.

Edited by: Benjamin Smith
Reviewed by: two anonymous referees

References

Albert, M. R. and Hardy, J. P.: Ventilation experiments in a seasonal snow cover, in: Biogeochemistry of Seasonally Snow-Covered Catchments, IAHS Publ. 228, edited by: Tonnessen, K. A., Williams, M. W., and Tranter, M., IAHS Press, Wallingford, UK, 41–49, 1995.

Calonne, N., Geindreau, C., Flin, F., Morin, S., Lesaffre, B., Rolland du Roscoat, S., and Charrier, P.: 3-D image-based numerical computations of snow permeability: links to specific surface area, density, and microstructural anisotropy, The Cryosphere, 6, 939–951, https://doi.org/10.5194/tc-6-939-2012, 2012.

Casado, M., Landais, A., Masson-Delmotte, V., Genthon, C., Kerstel, E., Kassi, S., Arnaud, L., Picard, G., Prie, F., Cattani, O., Steen-Larsen, H.-C., Vignon, E., and Cermak, P.: Continuous measurements of isotopic composition of water vapour on the East Antarctic Plateau, Atmos. Chem. Phys., 16, 8521–8538, https://doi.org/10.5194/acp-16-8521-2016, 2016.

Ciais, P. and Jouzel, J.: Deuterium and oxygen 18 in precipitation: Isotopic model, including mixed-cloud processes, J. Geophys. Res., 99, 16793–16803, https://doi.org/10.1029/94JD00412, 1994.

Colbeck, S. C.: Air movement in snow due to windpumping, J. Glaciol., 35, 209–213, 1989.

Craig, H. and Gordon, L. I.: Deuterium and oxygen 18 variations in the ocean and marine atmosphere, in: Proc. Stable Isotopes in Oceanographic Studies and Paleotemperatures, edited by: Toniorgi, E., Spoleto, Italy, 9–130, 1964.

Cuffey, K. M. and Steig, E. J.: Isotopic diffusion in polar firn: implications for interpretation of seasonal climate parameters in ice-core records, with emphasis on central Greenland, J. Glaciol., 44, 273–284, 1998.

Cuffey, K. M., Alley, R. B., Grootes, P. M., Bolzan, J. M., and Anandakrishnan, S.: Calibration of the Delta-O-18 isotopic paleothermometer for central Greenland, using borehole temperatures, J. Glaciol., 40, 341–349, 1994.

Dansgaard, W.: Stable isotopes in precipitation, Tellus, 16, 436–468, 1964.

Ebner, P. P., Grimm, S., Schneebeli, M., and Steinfeld, A.: An instrumented sample holder for time-lapse micro-tomography measurements of snow under advective conditions, Geosci. Instrum. Meth., 3, 179–185, https://doi.org/10.5194/gi-3-179-2014, 2014.

Ebner, P. P., Schneebeli, M., and Steinfeld, A.: Tomography-based monitoring of isothermal snow metamorphism under advective conditions, The Cryosphere, 9, 1363–1371, https://doi.org/10.5194/tc-9-1363-2015, 2015a.

Ebner, P. P., Andreoli, C., Schneebeli, M., and Steinfeld, A.: Tomography-based characterization of ice–air interface dynamics of temperature gradient snow metamorphism under advective conditions, J. Geophys. Res.-Earth, 120, 2437–2451, https://doi.org/10.1002/2015JF003648, 2015b.

Ebner, P. P., Schneebeli, M., and Steinfeld, A.: Metamorphism during temperature gradient with undersaturated advective airflow in a snow sample, The Cryosphere, 10, 791–797, https://doi.org/10.5194/tc-10-791-2016, 2016.

EPICA Members: Eight glacial cycles from an Antarctic ice core, Nature, 429, 623–628, https://doi.org/10.1038/nature02599, 2004.

Gjessing, Y. T.: The filtering effect of snow, in: Isotopes and Impurities in Snow and Ice Symposium, edited by: Oeschger, H., Ambach, W., Junge, C. E., Lorius, C., and Serebryanny, L., IASHAISH Publication, Dorking, 118, 199–203, 1977.

Grootes, P. M., Steig, E., and Stuiver, M.: Taylor Ice Dome study 1993–1994: an ice core to bedrock, Antarct. J. US, 29, 79–81, 1994.

Fisher, D. A. and Koerner, R.: The effect of wind on d(18O) and accumulation given an inferred record of seasonal d amplitude from the Agassiz ice cap, Ellesmere island, Canada, Ann. Glaciol., 10, 34–37, 1988.

Fisher, D. A. and Koerner, R.: Signal and noise in four ice-core records from the Agassiz ice cap, Ellesmere Island, Canada: details of the last millennium for stable isotopes, melt and solid conductivity, Holocene, 4, 113–120, https://doi.org/10.1177/095968369400400201, 1994.

Fisher, D. A., Koerner, R. M., Paterson, W. S. B., Dansgaard, W., Gundestrup, N., and Reeh, N.: Effect of wind scouring on climatic records from ice-core oxygen-isotope profiles, Nature, 301, 205–209, https://doi.org/10.1038/301205a0, 1983.

Friedman, I., Benson, C., and Gleason, J.: Isotopic changes during snow metamorphism, in: Stable Isotope Geochemistry: A Tribute to Samuel Epstein, edited by: O'Neill, J. R. and Kaplan, I. R., Geochemical Society, Washington, D. C., 211–221, 1991.

Haussener, S., Gergely, M., Schneebeli, M., and Steinfeld, A.: Determination of the macroscopic optical properties of snow based on exact morphology and direct pore-level heat transfer modeling, J. Geophys. Res., 117, 1–20, https://doi.org/10.1029/2012JF002332, 2012.

He, H. and Smith, R. B.: An advective-diffusive isotopic evaporation-condensation model, J. Geophys. Res., 104, 18619–18630, https://doi.org/10.1029/1999JD900335, 1999.

Helsen, M. M., van de Wal, R. S. W., van den Broeke, M. R., van As, D., Meijer, H. A. J., and Reijmer, C. H.: Oxygen isotope variability in snow from western Dronning Maud Land, Antarctica and its relation to temperature, Tellus, 57, 423–435, 2005.

Helsen, M. M., van de Wal, R. S. W., van den Broeke, M. R., Masson-Delmotte, V., Meijer, H. A. J., Scheele, M. P., and Werner, M.: Modeling the isotopic composition of Antarctic snow using backward trajectories: Simulation of snow pit records,J. Geophys. Res., 111, D15109, https://doi.org/10.1029/2005JD006524, 2006.

Helsen, M. M., van de Wal, R. S. W., and van den Broeke, M. R.: The isotopic composition of present-day Antartic snow in a Lagrangian simulation, J. Climate, 20, 739–756, 2007.

Hendricks, M. B., DePaolo, D. J., and Cohen, R. C.: Space and time variation of δ^{18}O and δD in precipitation: can paleotemperature be estimated from ice cores?, Global Biogeochem. Cy., 14, 851–861, https://doi.org/10.1029/1999GB001198, 2000.

Horita, J., Rozanski, K., and Cohen, S.: Isotope effects in the evaporation of water: a status report of the Craig-Gordon model, Isot. Environ. Health Sci., 44, 23–49, https://doi.org/10.1080/10256010801887174, 2008.

Hoshina, Y., Fujita, K., Nakazawa, F., Iizuka, Y., Miyake, T., Hirabayashi, M., Kuramoto, T., Fujita, S., and Motoyama, H.: Effect of accumulation rate on water stable isotopes of near-surface snow in inland Antarctica. J. Geophys. Res.-Atmos., 119, 274–283, https://doi.org/10.1002/2013JD020771, 2014.

Hoshina, Y., Fujita, K., Iizuka, Y., and Motoyama, H.: Inconsistent relations among major ions and water stable isotopes in Antartica snow under different accumulation environments, Polar Sci., 10, 1–10, https://doi.org/10.1016/j.polar.2015.12.003, 2016.

Johnsen, S. J.: Stable isotope homogenization of polar firn and ice, in: Isotopes and Impurities in Snow and Ice, Proceeding of the Grenoble Symposium, August/September 1975, IAHS AISH Publication, 118, Grenoble, France, 210–219, 1997.

Johnsen, S. J., Clausen, H. B., Cuffey, K. M., Hoffman, G., Schwander, J., and Creyts, T.: Diffusion of stable isotopes in polar firn and ice: the isotope effect in firn diffusion, in: Physics of Ice Core Records, edited by: Hondoh, T., Hokkaido University Press, Sapporo, Japan, 121–140, 2000.

Johnsen, S. J., Dahl-Jensen, D., Gundestrup, N., Steffensen, J. P., Clausen, H. B., Miller, H., Masson-Delmotte, V., Sveinbjörnsdottir A. E., and White, J.: Oxygen isotope and palaeotemperature records from six Greenland ice-core stations: Camp Century, DYE-3, GRIP, GISP2, Renland and NorthGRIP, J. Quaternary Sci., 16, 299–307, https://doi.org/10.1002/jqs.622, 2001.

Jouzel, J. and Merlivat, L.: Deuterium and oxygen 18 in precipitation: modeling of the isotopic effects during snow formation, J. Geophys. Res., 89, 11749–11757, https://doi.org/10.1029/JD089iD07p11749, 1984.

Jouzel, J., Merlivat, L., Petit, J. R., and Lorius, C.: Climatic information over the last century deduced from a detailed isotopic record in the South Pole snow, J. Geophys. Res., 88, 2693–2703, https://doi.org/10.1029/JC088iC04p02693, 1983.

Jouzel, J., Alley, R. B., Cuffey, K. M., Dansgaard, W., Grootes, P., Hoffmann, G., Johnsen, S. J., Koster, R. D., Peel, D., Shuman, C. A., Stievenard, M., Stuiver, M., and White, J.: Validity of the temperature reconstruction from water isotopes in ice cores, J. Geophys. Res., 102, 26471–26487, https://doi.org/10.1029/97JC01283, 1997.

Jouzel, J., Vimeux, F., Caillon, N., Delaygue, G., Hoffman, G., Masson-Delmotte, V., and Parrenin, F.: Magnitude of isotope/temperature scaling for interpretation of central Antarctic ice cores, J. Geophys. Res., 108, 1–6, https://doi.org/10.1029/2002JD002677, 2003.

Kaempfer, T. U. and Schneebeli, M. Observation of isothermal metamorphism of new snow and interpretation as a sintering process, J. Geophys. Res., 112, 1–10, https://doi.org/10.1029/2007JD009047, 2007.

Krinner, G. and Werner, M.: Impact of precipitation seasonality changes on isotopic signals in polar ice cores: A multi-model analysis, Earth Planet. Sc. Lett., 216, 525–538, https://doi.org/10.1016/S0012-821X(03)00550-8, 2003.

Lorius, C., Merlivat, L., Jouzel, J., and Pourchet, M.: A 30,000-yr isotope climatic record from Antarctica ice, Nature, 280, 644–648, https://doi.org/10.1038/280644a0, 1979.

Löwe H., Spiegel, J. K., and Schneebeli, M.: Interfacial and structural relaxations of snow under isothermal conditions, J. Glaciol., 57, 499–510, 2011.

Masson-Delmotte, V., Steen-Larsen, H. C., Ortega, P., Swingedouw, D., Popp, T., Vinther, B. M., Oerter, H., Sveinbjornsdottir, A. E., Gudlaugsdottir, H., Box, J. E., Falourd, S., Fettweis, X., Gallée, H., Garnier, E., Gkinis, V., Jouzel, J., Landais, A., Minster, B., Paradis, N., Orsi, A., Risi, C., Werner, M., and White, J. W. C.: Recent changes in north-west Greenland climate documented by NEEM shallow ice core data and simulations, and implications for past-temperature reconstructions, The Cryosphere, 9, 1481–1504, https://doi.org/10.5194/tc-9-1481-2015, 2015.

Merlivat, L. and Jouzel, J.: Global climatic interpretation of the deuterium-oxygen 18 relationship for precipitation, J. Geophys. Res., 84, 5029–5033, https://doi.org/10.1029/JC084iC08p05029, 1979.

Neumann, T. A.: Effects of firn ventilation on geochemistry of polar snow, PhD thesis, University of Washington, Washington, USA, 2003.

Neumann, T. A. and Waddington, E. D.: Effects of firn ventilation on isotopic exchange, J. Glaciol., 50, 183–194, 2004.

Neumann, T. A., Albert, M. R., Lomonaco, R., Engel, C., Courville, Z., and Perron, F.: Experimental determination of snow sublimation rate and stable-isotopic exchange, Ann. Glaciol., 49, 1–6, 2008.

Otsu, N.: A threshold selection method from gray-level histograms, IEEE T. Syst. Man Cyb., 9, 62–66, 1979.

Penna, D., Stenni, B., Šanda, M., Wrede, S., Bogaard, T. A., Michelini, M., Fischer, B. M. C., Gobbi, A., Mantese, N., Zuecco, G., Borga, M., Bonazza, M., Sobotková, M., Čejková, B., and Wassenaar, L. I.: Technical Note: Evaluation of between-sample memory effects in the analysis of δ^2H and δ^{18}O of water samples measured by laser spectroscopes, Hydrol. Earth Syst. Sci., 16, 3925–3933, https://doi.org/10.5194/hess-16-3925-2012, 2012.

Persson, A., Langen, P. L., Ditlevsen, P., and Vinther, B. M.: The influence of precipitation weighting on interannual variability of stable water isotopes in Greenland, J. Geophys. Res.-Atmos., 116, 1–13, https://doi.org/10.1029/2010JD015517, 2011.

Petit, J. R., Jouzel, J., Raynaud, D., Barkov, N. I., Barnola, J.-M., Basile, I., Bender, M., Chappellaz, J., Davis, M., Delaygue, G., Delmotte, M., Kotlyakov, V. M., Legrand, M., Lorius, C., Pépin, L., Ritz, C., Saltzman, E. S., and Stievenard, M.: Climate and atmospheric history of the past 420,000 years from the Vostok ice core, Antarctica, Nature, 399, 429–436, https://doi.org/10.1038/20859, 1999.

Pinzer, B. R. and Schneebeli, M.: Snow metamorphism under alternating temperature gradients: morphology and recrystallization in surface snow, Geophys. Res. Lett., 36, L23503, https://doi.org/10.1029/2009GL039618, 2009.

Pinzer, B. R., Schneebeli, M., and Kaempfer, T. U.: Vapor flux and recrystallization during dry snow metamorphism under a steady temperature gradient as observed by time-lapse micro-tomography, The Cryosphere, 6, 1141–1155, https://doi.org/10.5194/tc-6-1141-2012, 2012.

Ramseier, R. O: Self-diffusion of tritium in natural and synthetic ice monocrystals, J. Appl. Phys., 38, 2553–2556, 1967.

Ritter, F., Steen-Larsen, H. C., Werner, M., Masson-Delmotte, V., Orsi, A., Behrens, M., Birnbaum, G., Freitag, J., Risi, C., and Kipfstuhl, S.: Isotopic exchange on the diurnal scale between near-surface snow and lower atmospheric water vapor at Kohnen station, East Antarctica, The Cryosphere, 10, 1647–1663, https://doi.org/10.5194/tc-10-1647-2016, 2016.

Schleef, S., Jaggi, M., Löwe H., and Schneebeli, M.: Instruments and methods: an improved machine to produce nature-identical snow in the laboratory, J. Glaciol., 60, 94–102, 2014.

Sjolte, J., Hoffmann, G., Johnsen, S. J., Vinther, B. M., Masson-Delmotte, V., and Sturm, C.: Modeling the water isotopes in Greenland precipitation 1959–2001 with the meso-scale model remo-iso, J. Geophys. Res., 116, 1–22, https://doi.org/10.1029/2010JD015287, 2011.

Sokratov, S. A. and Golubev, V. N.: Snow isotopic content change by sublimation. J. Glaciol., 55, 823–828, 2009.

Steen-Larsen, H. C., Masson-Delmotte, V., Sjolte, J., Johnsen, S. J., Vinther, B. M., Breon, F. M., Clausen, H. B., Dahl-Jensen, D., Falourd, S., Fettweis, X., Gallee, H., Jouzel, J., Kageyama, M., Lerche, H., Minster, B., Picard, G., Punge, H. J., Risi, C., Salas, D., Schwander, J., Steffen, K., Sveinbjornsdottir, A. E., Svensson, A., and White, J.: Understanding the climatic signal in the water stable isotope records from the neem shallow firn/ice cores in northwest Greenland, J. Geophys. Res.-Atmos., 116, 1–20, https://doi.org/10.1029/2010JD014311, 2011.

Steen-Larsen, H. C., Johnsen, S. J., Masson-Delmotte, V., Stenni, B., Risi, C., Sodemann, H., Balslev-Clausen, D., Blunier, T., Dahl-Jensen, D., Ellehøj, M. D., Falourd, S., Grindsted, A., Gkinis, V., Jouzel, J., Popp, T., Sheldon, S., Simonsen, S. B., Sjolte, J., Steffensen, J. P., Sperlich, P., Sveinbjörnsdóttir, A. E., Vinther, B. M., and White, J. W. C.: Continuous monitoring of summer surface water vapor isotopic composition above the Greenland Ice Sheet, Atmos. Chem. Phys., 13, 4815–4828, https://doi.org/10.5194/acp-13-4815-2013, 2013.

Steen-Larsen, H. C., Masson-Delmotte, V., Hirabayashi, M., Winkler, R., Satow, K., Prié, F., Bayou, N., Brun, E., Cuffey, K. M., Dahl-Jensen, D., Dumont, M., Guillevic, M., Kipfstuhl, S., Landais, A., Popp, T., Risi, C., Steffen, K., Stenni, B., and Sveinbjörnsdottír, A. E.: What controls the isotopic composition of Greenland surface snow?, Clim. Past, 10, 377–392, https://doi.org/10.5194/cp-10-377-2014, 2014a.

Steen-Larsen, H. C., Sveinbjörnsdottir, A. E., Peters, A. J., Masson-Delmotte, V., Guishard, M. P., Hsiao, G., Jouzel, J., Noone, D., Warren, J. K., and White, J. W. C.: Climatic controls on water vapor deuterium excess in the marine boundary layer of the North Atlantic based on 500 days of in situ, continuous measurements, Atmos. Chem. Phys., 14, 7741–7756, https://doi.org/10.5194/acp-14-7741-2014, 2014b.

Sturm, M. and Johnson, J. B.: Natural convection in the subarctic snow cover, J. Geophys. Res., 96, 11657–11671, https://doi.org/10.1029/91JB00895, 1991.

Town, M. S., Warren, S. G., Walden, V. P., and Waddington, E. D.: Effect of atmospheric water vapor on modification of stable isotopes in near-surface snow on ice sheets, J. Geophys. Res.-Atmos., 113, 1–16, https://doi.org/10.1029/2008JD009852, 2008.

van der Wel, G., Fischer, H., Oerter, H., Meyer, H., and Meijer, H. A. J.: Estimation and calibration of the water isotope differential diffusion length in ice core records, The Cryosphere, 9, 1601–1616, https://doi.org/10.5194/tc-9-1601-2015, 2015.

Waddington, E. D., Cunningham, J., and Harder, S. L.: The effects of snow ventilation on chemical concentrations, in: Chemical Exchange Between the Atmosphere and Polar Snow, edited by: Wolff, E. W. and Bales, R. C., Springer, Berlin, NATO ASI Series, 43, 403–452, 1996.

Waddington, E. D., Steig, E. J., and Neumann, T. A.: Using characteristic times to assess whether stable isotopes in polar snow can be reversibly deposited, Ann. Glaciol., 35, 118–124, 2002.

Werner, M., Langebroek, P. M., Carlsen, T., Herold, M., and Lohmann, G.: Stable water isotopes in the ECHAM5 general circulation model: Toward high-resolution isotope modeling on a global scale, J. Geophys. Res.-Atmos., 116, D15109, https://doi.org/10.1029/2011JD015681, 2011.

White, J. W., Barlow, L. K., Fisher, D., Grootes, P., Jouzel, J., Johnsen, S. J., Stuiver, M., and Clausen, H.: The climate signal in the stable isotopes of snow from Summit, Greenland: Results of comparisons with modern climate observations, J. Geophys. Res., 102, 26425–26439, https://doi.org/10.1029/97JC00162, 1997.

Zermatten, E., Schneebeli, M., Arakawa, H., and Steinfeld, A.: Tomography-based determination of porosity, specific area and permeability of snow and comparison with measurements, Cold Reg. Sci. Technol., 97, 33–40, https://doi.org/10.1016/j.coldregions.2013.09.013, 2014.